

Fabrication of a 3D hair follicle-like hydrogel by soft lithography

Jing Pan,¹ Sui Yung Chan,¹ John E. A. Common,² Shahrouz Amini,³ Ali Miserez,³ E. Birgitte Lane,² Lifeng Kang¹

¹Department of Pharmacy, National University of Singapore, 18 Science Drive 4, Singapore 117543, Singapore

²Institute of Medical Biology, Immunos, 8A Biomedical Grove, Singapore 138648, Singapore

³School of Materials Science and Engineering and School of Biological Sciences, Nanyang Technological University, Singapore 639798, Singapore

Received 1 September 2012; revised 8 January 2013; accepted 22 January 2013

Published online in Wiley Online Library (wileyonlinelibrary.com). DOI: 10.1002/jbm.a.34628

Abstract: Hair follicle transplantation is often used in the treatment of androgenetic alopecia (AGA). However, the only source of hair follicles is from human donors themselves, which limits the application of this approach. One possible solution is to reconstitute hair follicle from dissociated cells. Currently, a number of microscale technologies have been developed to create size and shape controlled microenvironments in tissue engineering. Photopolymerizable PEGDA hydrogels are often selected as promising scaffolds in engineered microtissues due to their biocompatibility and adjustable mechanical properties. Here, we fabricated an array of PEGDA microwells with center islets that mimic the architecture of human hair follicles using soft lithography. Dermal

and epithelial cells were seeded in different compartments of the microstructured mould to mimic mesenchymal and epithelial compartmentalization in native hair follicles. We demonstrated that these compartmentalized microstructures support cell proliferation and cell survival over 14 days, and spreading of dermal fibroblasts was observed. This hydrogel micromould provides a potentially useful tool for engineering 3D hair follicle-mimicking complex cultures *in vitro*. © 2013 Wiley Periodicals, Inc. *J Biomed Mater Res Part A*: 00A:000–000, 2013.

Key Words: hair follicle, hydrogel, microstructure, soft lithography, tissue engineering

How to cite this article: Pan J, Chan SY, Common JEA, Amini S, Miserez A, Lane EB, Kang L. 2013. Fabrication of a 3D hair follicle-like hydrogel by soft lithography. *J Biomed Mater Res Part A* 2013;00A:000–000.

INTRODUCTION

The human hair cycle consists of three main phases—anagen (growth phase), catagen (involutional/regression phase), and telogen (resting phase). The anagen phase of human scalp typically lasts for 2–6 years which is the determinative factor of hair length. Catagen usually lasts for 2–3 weeks, while telogen 3 months. Changes in the hair cycle result in hair growth disorders,¹ the most frequent being androgenetic alopecia (AGA), commonly known as male pattern baldness.² AGA affects approximately 50% of men and 20–53% of women by age 50 years.³ Currently, the available treatment for AGA involves the use of drugs such as minoxidil and finasteride.^{4,5} However, hair fall resumes upon withdrawal of the drugs and side effects accompany the treatment. An alternative solution to treat AGA is using surgical procedure to transplant grafts containing hair follicles.⁶ Although this method is effective in hair regeneration, there is no other alternative of harvesting hair follicles other than from human donors.⁷

To this end, several studies have attempted to reconstitute hair follicle-like structures from dissociated cells. In humans, hair follicle regeneration is a result of epithelial–

mesenchymal cell interactions, which is widely accepted and considered as essential for hair follicle morphogenesis.^{8,9} Signals from the condensed mesenchymal cells in the dermal papilla (DP) are thought to induce the proliferation of epithelial cells. The proliferated epithelial cells grow downward to encapsulate the condensed mesenchymal cells, followed by hair follicle formation.¹⁰ Previous studies have shown hair follicle-like structures can form by combining a population of hair follicle inductive dermal cells with a population of follicular epidermal cells in an animal model.^{11,12} Using homospecific mouse or rat cells or heterospecific mouse–rat combinations, normal appearing hairs can be reconstituted.^{12,13} Plucked human hair follicles can also be maintained in a growing state for some days in tissue culture.¹⁴ However, human mesenchymal dermal papilla and epithelial hair follicle cells cannot be recombined to form normal hair follicles *de novo* in tissue culture because the human mesenchymal cells lose their hair inductivity during culture and human epidermal cells may not maintain sufficient differentiation ability over time.^{13,15,16} So far, the closest structures to human hair follicle have been obtained by co-grafting

Additional Supporting Information may be found in the online version of this article.

Correspondence to: L. Kang; e-mail: lkang@nus.edu.sg

Contract grant sponsor: The Singapore National Medical Research Council (NMRC); contract grant number: NIG09MAY029

foreskin-derived human keratinocytes and murine DP cells onto nude mice¹³. However, hair follicles formed in xenografts of human and murine cell components are not suitable for hair transplantation due to the immune rejection.^{17,18} The failure to form better differentiated and organized follicles is believed to be due to the lack of communication between the mesenchymal and epithelial cells.^{3,19}

With the increasing progress in microscale technologies, new approaches have been developed to investigate cell behaviors in microenvironments for cellular biology and tissue engineering applications.²⁰ Microscale technologies such as soft lithography, photolithography, flow lithography, and bioprinting have enabled the construction of diverse synthetic microstructures to incorporate cells.^{21–26} Microstructures are expected to provide cells with a suitable microenvironment, sufficient nutrient transport, and mechanical integrity.^{20,27,28} In particular, three dimensional (3D) microstructures can be readily made using photocrosslinkable polymers with adjustable mechanical properties, microarchitecture, and alterable chemical compositions.^{23,29} Soft lithography, which employs elastomeric stamps fabricated from patterned silicon wafers to print or mold materials, is commonly used in 3D microstructure fabrication.³⁰

In this study, microstructured scaffolds were fabricated in which hair follicle inductive dermal cells can be positioned and grown close to, but separated from epidermal cell populations by soft lithography. The mould resembles the physiological architecture of hair follicle [Fig. 1(A)]. Poly(dimethylsiloxane) (PDMS) stamps were fabricated from patterned silicon masters and then the stamps were employed to mold poly(ethylene glycol) diacrylate (PEGDA) microwells with center islets on a glass slide by UV crosslinking [Fig. 1(B)]. Epithelial cells and dermal cells were immobilized in different locations of the microstructure for tissue culturing. Such a scaffold can serve as a potential platform for hair follicle regeneration *in vitro*.

EXPERIMENTAL

Master fabrication

Photomasks were designed using AutoCAD 2010 and printed on chromium coated soda lime glasses at Infinite Graphics PTE LTD (Singapore). Silicon wafers were spin-coated with the epoxy negative photoresist SU-8 2050 (MicroChem Corp., Newton, MA) at 2200 rpm, yielding the desired film thickness of 50 μm . Wafers were soft-baked at 65°C for 1 min, followed by a second baking at 95°C for 10 min. For crosslinking of the photoresist, the coated wafers were exposed to UV light of 350–400 nm for 65 s through a photomask on a single-side mask aligner (SVC, Model H94-25). Subsequently, the wafers were post-exposure baked at 65°C for 1 min and then at 95°C for 6 min. The photoresist-patterned silicon masters were developed using SU-8 developer, rinsed with isopropyl alcohol for 10 s, and air dried with pressurized nitrogen. The pattern of protruding rods was analyzed using an optical microscope equipped on the aligner. For secondary spin-coating, patterned silicon masters were spin-coated with negative photoresist SU-8 2075 (MicroChem Corp., Newton, MA) at

1000 rpm, yielding the desired film thickness about 200 μm . Wafers were soft-baked at 65°C for 7 min, followed by a second soft-baking at 95°C for 60 min. After aligning the patterned master with the second photomask by the crosses on each of them, the coated wafers were exposed to UV light of 350–400 nm for 90 s through the second photomask by using the aligner. Subsequently, the wafers were post-exposure baked at 65°C for 6 min and then at 95°C for 15 min. The photoresist-patterned silicon masters were developed using SU-8 developer, rinsed with isopropyl alcohol for 10 s, and air dried with pressurized nitrogen. Four different dimensions of microwells were obtained with center islets in accordance with the design of photomasks (50 μm with 16 μm islet, 100 μm with 33 μm islet, 200 μm with 66 μm islet, and 400 μm with 133 μm islet).

PDMS-stamp fabrication

Poly(dimethylsiloxane) (PDMS) stamps were fabricated by curing a 10:1 mixture of silicone elastomer base solution and curing agent Sylgard 184 (Dow Corning Corporation, Midland, USA) on a patterned silicon master. The PDMS elastomer solution was degassed for 20–30 min in a vacuum chamber and cured at 70°C for 2–4 h before the PDMS stamps were peeled from the silicon masters. The generated PDMS replicas had patterns corresponding to the silicon master with protruding columns and were subsequently used for molding of PEGDA microwells.

To identify outlines of PDMS stamps, a slice of the PDMS stamp was cut using a blade and treated the surface by using oxygen plasma for 3 min (Harrick Scientific, USA). Then, the slice was immersed in 5 $\mu\text{g}/\text{ml}$ Rhodamine B (Alfa Aesar, Lancaster, UK) and observed under a fluorescent microscope (Nikon Ti, Japan, ex: 545–565 nm).

Microwell fabrication

Microwell arrays were fabricated using UV-photocrosslinkable PEGDA (Aldrich Chemistry, USA and Jenkem Technology, USA) of different average molecular weights (MWs; 575, 700, and 3500 Da) mixed in a 0.2% (w/v) ratio of the photoinitiator 2-hydroxy-4'-(2-hydroxy-ethoxy)-2-methylpropiophenone (Irgacure 2959, Aldrich Chemistry, USA) on a 3-(trimethoxysilyl) propyl methacrylate (TMS-PMA, Sigma, USA) treated glass slide. A patterned PDMS stamp was placed on an evenly distributed film of precursor solution on a glass slide. To optimize the conditions for PEGDA hydrogel photopolymerization, we determined the minimum duration of UV exposure required for the formation of designed microwell arrays at various UV intensities. After polymerization, the PDMS stamp was peeled from the substrate. All photopolymerizations were performed using the OmniCure[®] Series 2000 curing station (320–500 nm; Lumen Dynamics, Canada).

Microwell stability

To find stable microwell arrays molded on TMS-PMA-treated glass slides, prepolymer solutions of various PEGDA concentrations (10, 20, 40, and 80% w/v) were used to fabricate microwell arrays. The stability of microwells on the glass

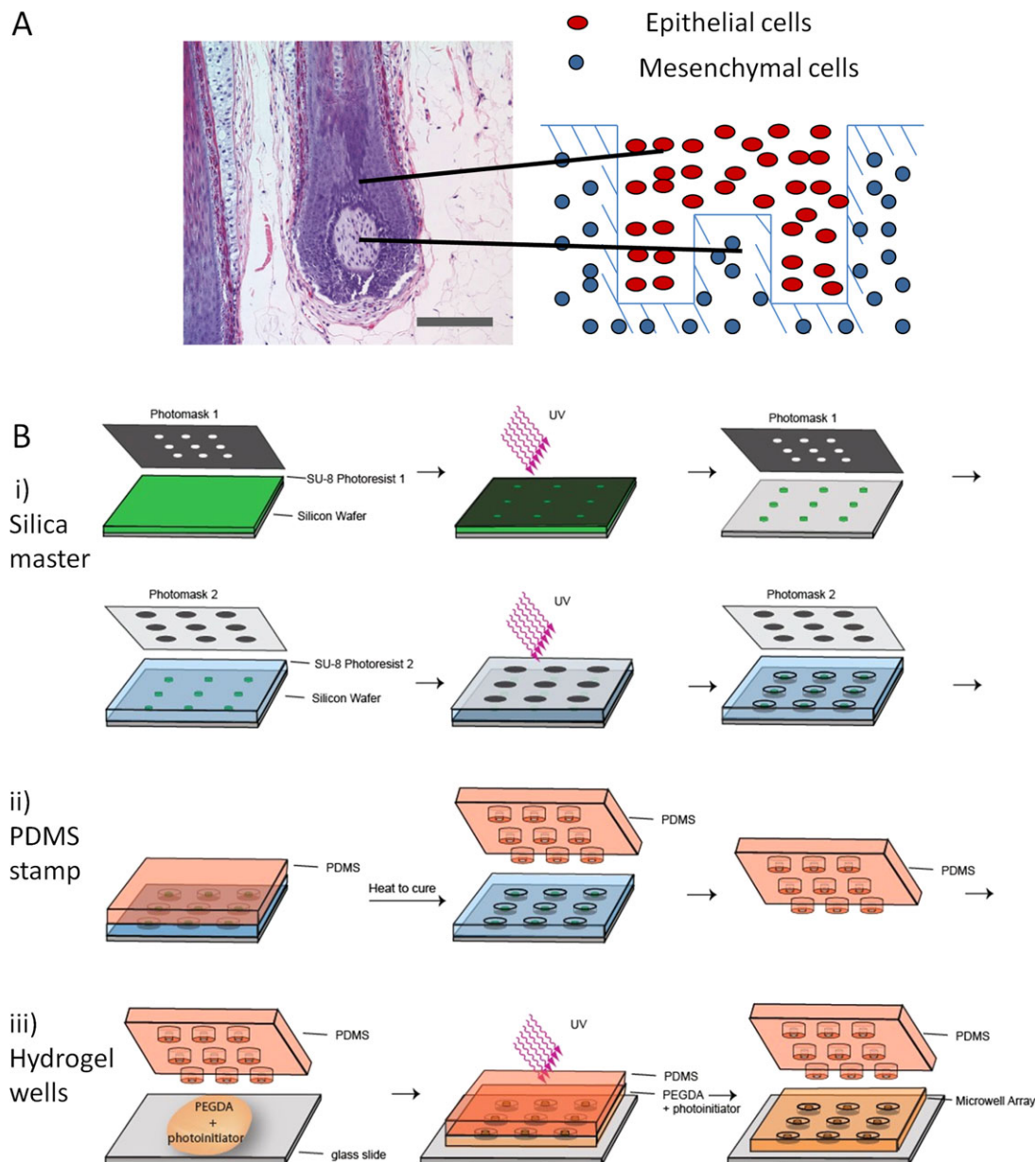


FIGURE 1. Schematic representation of hair follicle-like mould fabrication. A: There are two types of cells which are necessary for hair follicle generation. Blue dots represent mesenchymal cells which can induce the proliferation of epithelial cells (red dots). The scale bar represents 100 μm . (David A. Whiting. *Histology of the Human Hair Follicle*. In: Ulrike Blume-Peytavi, Antonella Tosti, David A. Whiting, Ralph M. Trüeb, editor. *Hair Growth and Disorders*: Springer-Verlag Berlin Heidelberg; 2008. p 107–123. With kind permission of Springer Science+Business Media.) B: Microwell fabrication: (i) silicon master manufacturing, (ii) PDMS stamp production, and (iii) hydrogel wells fabrication. [Color figure can be viewed in the online issue, which is available at wileyonlinelibrary.com.]

slides was assessed by immersing microarrays in phosphate-buffered saline (PBS, Vivantis, KL, Malaysia) in 37°C, 5% CO₂ humidified incubator and analyzing the integrity of the arrays over time. In all cases, dilutions were made in 1× PBS. Experiments were conducted in triplicates.

Mechanical testing

Polymerization was performed as described for microwell fabrication. Samples were incubated in PBS at 37°C, 5% CO₂ humidified incubator for 24 h to make gels swell to reach equilibrium.³¹ Young's modulus of PEGDA hydrogels

were obtained by probing flat surfaces by nanoindentation, using a Triboindenter (Hysitron, Minneapolis, MN). We chose a spherical indenter tip ($R \sim 50 \mu\text{m}$) for nanoindentation studies, using a peak load of 25 μN , a loading/unloading rate of 5 $\mu\text{N/s}$, and a holding time at peak load of 2 s. The Young's modulus was determined as the slope of the linear region upon unloading. Sixteen indentation curves were performed within a 600 $\mu\text{m} \times 600 \mu\text{m}$ area at a lateral separation of 150 μm . During the nanoindentation test, the hydrogels were kept in PBS solution to avoid dehydration.

Cell culture

Human dermal fibroblast (HDF) and human adult low calcium high temperature (HaCaT) keratinocyte cells were manipulated under aseptic conditions and maintained in a humidified incubator at 37°C with a 5% CO₂ atmosphere. Media components were filtered through 0.22 μm pore Corning filter units (Corning Incorporated, USA). Culture media consisted of Dulbecco's modified Eagle's medium (DMEM, Invitrogen Corporation, USA) supplemented with 10% fetal bovine serum (FBS, Invitrogen Corporation, USA), 1% 10,000 U/mL penicillin and 10 mg/mL streptomycin (PAN-Biotech GmbH, Germany).

Cell seeding

Using a previously reported method, cells were seeded into the microwells.³² Briefly, 20 μL of cell media (1–12 million cells per mL) was pipetted along the edge of a microscopy glass coverslip which was then slowly wiped across a microwell array. The coverslip was wiped across the array at 1.0 mm/s and the array was placed in a humid enclosure to avoid evaporation of the isolated droplets in the microwells. Cell viability after seeding process was assessed using a Live/Dead stain kit (Invitrogen Corporation, USA). Cells were incubated in 4 μM ethidium homodimer (Ethd) and 2 μM calcein-AM in PBS for 10 min at 37°C. Live cells were stained green due to enzymatic conversion of the non-fluorescent cell-permeant calcein-AM to fluorescent calcein. Dead cells were stained red after binding of Ethd to nucleic acids of membrane-compromised cells. The number of cells was counted manually using ImageJ (<http://rsbweb.nih.gov/ij/>).

Cell encapsulation

To fabricate cell-laden microwells, HDF cells were trypsinized and mixed with 10% (w/v) PEGDA prepolymer solutions with different average MW (PEGDA 575, PEGDA 700, and PEGDA 3500) containing 0.2% (w/v) photoinitiator at 2×10^6 cells/mL. Then, following the microwell fabrication process, 60 μL cell suspensions were transferred on a TMS-PMA treated glass slide and a patterned PDMS stamp was placed on the cell suspension, followed by UV photocrosslinking. After photopolymerization, the cell-laden microgels were transferred into tissue culture petri-dishes containing DMEM culture medium. Cell-laden microgels were cultured over 14 days in a humidified incubator at 37°C with 5% CO₂ atmosphere and fed with medium every 2–3 days. Cell viability was assessed by the Live/Dead assay.

Cell distribution in 3D microstructure

Polymerization was performed as described for cell encapsulation. Immediately following hydrogel formation, glass slides with patterned microstructures were transferred in DMEM culture medium at 37°C with 5% CO₂ atmosphere for 1 h. Then, the cell-laden hydrogels were incubated in 4 μM Ethd and 2 μM calcein-AM in PBS for 30 min and the microwells were imaged using a Nikon SMZ 1500 stereomicroscope (Nikon, Japan) to characterize cell distribution in the 3D microstructure.

Statistics

Data were compared using ANOVA followed by Bonferroni's post-hoc test using a GraphPad Prism 5.0 software (San Diego, USA).

RESULTS AND DISCUSSION

Microwell fabrication

The silicon wafer was patterned with the photoresist SU-8 to form microwells with center islets resembling the architecture of hair follicles [Fig. 1(B)]. Four dimensions (50, 100, 200 and 400 μm) were chosen based on histological studies of the hair follicle, which showed that a human hair follicle is approximately 150–200 μm in diameter at its root.² The ratio between the diameter of the center islet and the diameter of the microwell is 1:3, since the diameter of the mesenchymal condense enclosed by hair matrix cells is nearly one third of the diameter of lower hair bulb. The side views of PDMS patterned from the silicon master were shown in Figure 2(A) (i–iv). The PDMS stamps filled with rhodamine B solutions showed the microwell diameters (MD), the microwell heights (MH), and the height of center islets (IH) [Fig. 2(A)]. Microwells of various diameters were fabricated from PEGDA precursor solutions by using these PDMS stamps [Fig. 2(B) (i–iv)]. As a widely used biomaterial, PEGDA is hydrophilic and photocrosslinkable.³³ In addition, the porous form of PEGDA hydrogel was reported not to confine the mobility of cells and support epithelial–mesenchymal cell interactions.²⁰ To increase the bonding of the polymer–glass interface, the glass substrates were acrylated using TMS-PMA. This surface treatment introduced terminal acrylate functional groups on the glass, providing anchoring sites for the PEG acrylates.³⁴

The design of microstructure may influence cell function. Eukaryotic cells contain geometry-sensing tools in their cytosol which recognize the change of membrane curvature.³⁵ Membrane curvature is closely related to cell growth, division, and movement.³⁶ In our study, although the microwell is not exactly the same as the architecture of hair follicle, our design follows the dimension of hair follicle and facilitates the cell distribution in a similar way to that in the hair follicle. In the early anagen, the mesenchymal cells lie beneath the epithelial cells while the rapidly proliferating epithelial cells enclose the mesenchymal cells. The use of the microstructure described here will immobilize these two types of cells at designated locations, which can better mimic their spatial relationship *in vivo*.

Microwell stability

To test the stability of microwells over time, the microwells were immersed in 1× PBS buffer and monitored daily. Microwells were deemed as “unstable” if they detached from the underlying glass slide. During the study, cracks developed in some microwell arrays but these cracks did not affect all microwells on an array. Hence, two different criteria were established to describe the microwell stability, namely “stability by counting” and “overall stability”. For overall stability, microwell arrays were deemed as “unstable” once one or more cracks or detachments occurred from

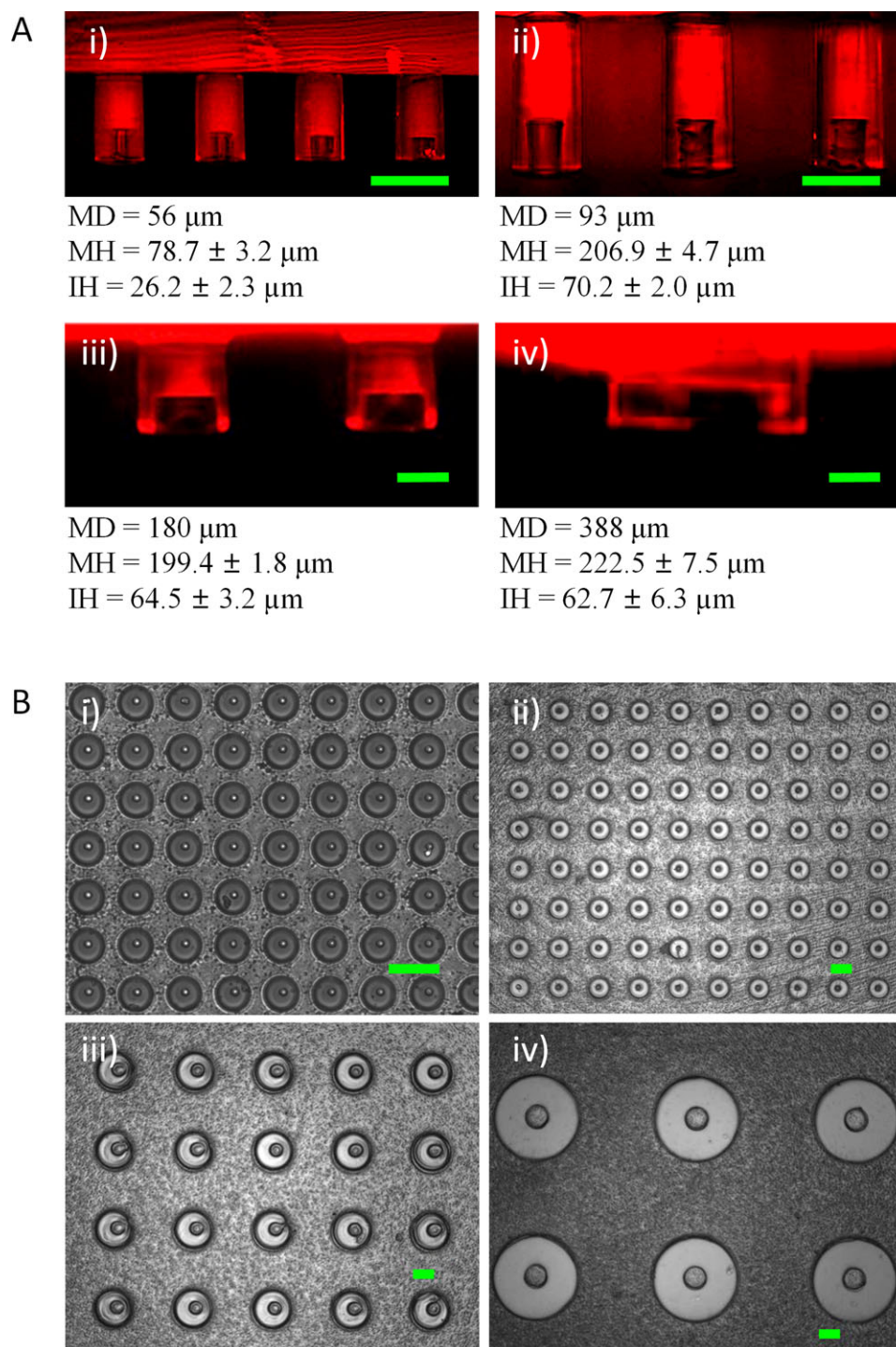


FIGURE 2. Different dimensions of PDMS stamps and corresponding hydrogel microwells. A: Cross-sectional images of PDMS stamps (i–iv microwell diameters: 56, 93, 180, and 388 μm) stained by rhodamine B, where MD represents microwell diameter; MH represents microwell height; IH represents islet height. B: i–iv: images of microwells with various diameters fabricated by 10% (w/v) PEGDA. All scale bars represent 100 μm . [Color figure can be viewed in the online issue, which is available at wileyonlinelibrary.com.]

underlying glass substrate [Supporting Information Fig. 1(A)]. Overall stability may be employed when the integrity of whole microwell arrays is essential in this study. For stability by counting, the number of individual damaged microwells was counted every day and the overall percentage of stable microwells was calculated [Supporting Information

Fig. 1(B)]. Partially detached microwell arrays were still useful if only a few microwells are damaged because of the cracks. Most microwells made of 80% (w/v) PEGDA solution detached partially when incubated in $1\times$ PBS for 1 or 2 days, while microwells made of 10 and 20% (w/v) PEGDA remained stable for up to 10 days. Microwells made of 40%

(w/v) PEGDA solution showed inconsistent stability for different dimensions of microwell arrays.

Diluted prepolymer solution [$<40\%$ (w/v) PEGDA] formed stable microwells. The reason for the results can be explained by the gel swelling upon exposure to an aqueous environment. When hydrophilic polymeric networks are placed in contact with water, they usually swell due to favorable thermodynamic interaction of macromolecular segments with water molecules.^{37–39} Thus, higher concentrations of prepolymer solutions [$\geq 40\%$ (w/v) PEGDA] allowed rapid water uptake and swelling which created stress across the glass–polymer interface and led to detachment of the microwell array. The results are consistent with those reported by Hannes-Christian Moeller et al.³⁷

Mechanical properties

To further understand the mechanical properties of microwell arrays, nanoindentation studies were performed to measure the stiffness of PEGDA hydrogels. After the stability test, only 10 and 20% (w/v) PEGDA were chosen for the cell-encapsulation study due to their high stability. Therefore, the stiffness of these hydrogels were measured. To assess the homogeneity of the hydrogel, the stiffness of microwell bottom and hydrogel surface were tested. Indentation results showed that there were no significant differences between the stiffness of microwell bottoms and hydrogel surfaces (Fig. 3). It was also shown that the Young's modulus of 20% (w/v) PEGDA was significantly higher than that of 10% (w/v) PEGDA, as increasing the PEGDA concentration increased the number of reactive diacrylate groups in the polymerization, thereby leading to increase crosslink densities of hydrogel samples.

Tissue culture

In this study, HDF and HaCaT cells were used instead of DP and primary keratinocytes which are involved in epithelial–mesenchymal interactions in the hair follicle in humans. The DP is a group of specialized dermal fibroblast cells, derived from the embryonic mesoderm.⁴⁰ However, compared with HDFs, papilla cells exhibit a shorter *in vitro* survival time and papilla cells may lose their hair inductivity during culture.¹³ It was reported that HDFs may also exert DP-like activity including hair inductivity.⁴¹ On the other hand, the immortalized HaCaT cell line was employed as a keratinocyte model in this study due to its ease of propagation and to establish our hydrogel tissue culturing system.⁴²

To fabricate complex tissues, co-culture of different cell types in physiologically relevant geometrical patterns is required. In addition, quantitative control of these cells within scaffold is also important.⁴³ The number of HDF cells in the gel was controlled by preparing different densities of cell suspensions prior to microwell fabrication. For the quantitative control of HaCaT cells, a wiping technique, established in our previous study, was employed.³² This wiping method produced relatively uniform distribution of cells in the microstructures and accurately predicted cell seeding densities.³² Using this method, we seeded various densities of HaCaT cells (1–12 million cells per mL) inside

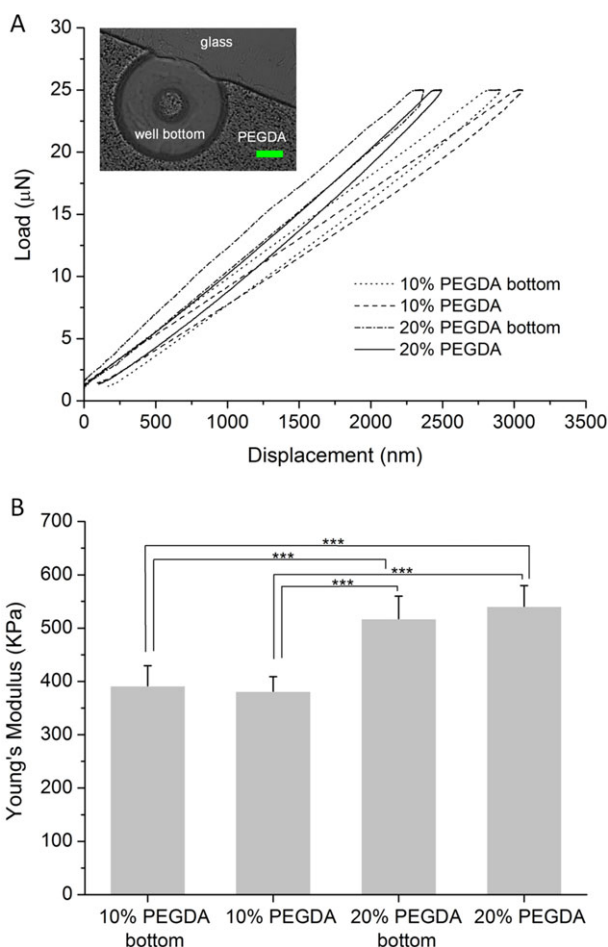


FIGURE 3. Mechanical properties of PEGDA hydrogels with varying gel percentage and thickness. A: Representative nanoindentation curves from 10% (w/v) PEGDA microwell bottom, 10% (w/v) PEGDA hydrogel, 20% (w/v) PEGDA microwell bottom, and 20% (w/v) PEGDA hydrogel. B: Young's modulus for 10% (w/v) PEGDA microwell bottom, 10% (w/v) PEGDA hydrogel, 20% (w/v) PEGDA microwell bottom, and 20% (w/v) PEGDA hydrogel. Young's modulus of 20% (w/v) PEGDA was significantly higher than that of 10% (w/v) PEGDA ($***p < 0.001$) while there were no significant differences between Young's modulus of microwell bottoms and surfaces for both concentrations of PEGDA. The scale bar represents 100 μm . [Color figure can be viewed in the online issue, which is available at wileyonlinelibrary.com.]

microwells [Fig. 4(A–E)]. Similar to previous study, the number of cells in the microwells increased with the cell seeding density [Fig. 4(F)]. The difference is that a broader range of cell densities was selected. Hence, this wiping method was verified to be also useful in high cell densities when more cells were retained within the microwells. From Figure 4(F), the linear least-squares fit has a slope of 4.00 for $d = 200 \mu\text{m}$ while the slope in previous study was 7.62 for $d = 229 \mu\text{m}$.³² This may be due to the difference in microwell diameters and patterns. The new design has a center islet in the middle of the microwell which may have influenced the capacity of the microwell in docking cells.

Some center islets were covered by HaCaT cells when initial cell solution concentration was increased to 12 million cells per mL. It was shown in Figure 4 that the number of

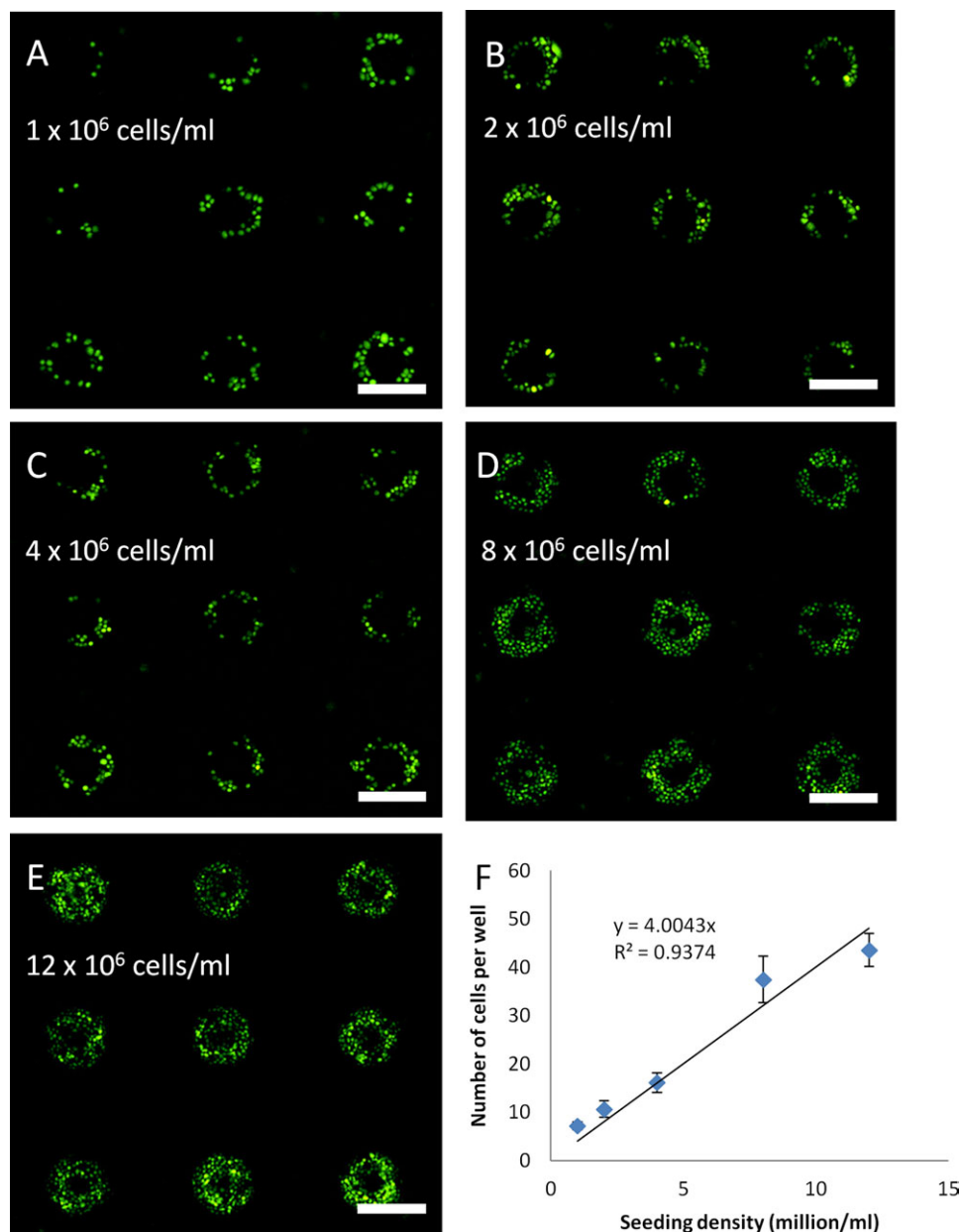


FIGURE 4. Various densities of HaCaT cells seeded on the top of microwell arrays. A–E: Representative images of HaCaT cells stained with calcein-AM fluorescent dye in the microwells with different cell seeding densities. F: The average number of cells per well increased with increasing initial cell concentration ($n = 3$). Scale bars represent 200 μm . [Color figure can be viewed in the online issue, which is available at wileyonlinelibrary.com.]

HaCaT cells increased with seeding cell density. The average number of cells per well at low seeding cell densities was tested because cells were discernible at such concentrations. For the actual biological studies, further increase of the seeding cell concentrations will be needed to ensure all center islets are covered by epithelial cells, using the linear relationship.

To test the cell compatibility with the moulds, the viability of HDF cells and HaCaT cells by Live/Dead assays was ascertained. From the results, HDF cells in the control group (before UV exposure) and the experimental group (after UV exposure) were all stained in green (live cells) and red

(dead cells) colors [Fig. 5(A)]. Cells encapsulated in the fabricated gels were uniformly distributed in 3D microstructures [Fig. 5(A-vi)]. The comparison of cell viability before and after polymerization showed that the fabrication process decreased cell viability [Fig. 5(B-i)]. Cell viability varied with different PEGDAs after polymerization. PEGDA 3500 was the least toxic to the cell and cell viability was 88.4% ($\pm 2.6\%$, $n = 3$) after photocrosslinking while cell viability of PEGDA 575 and PEGDA 700 were 70.4 ($\pm 1.8\%$, $n = 3$), and 73.8 ($\pm 2.9\%$, $n = 3$) respectively.

The synthesis of cell-laden microgels from cell-monomer mixture requires UV exposure, photoinitiator, and PEGDA

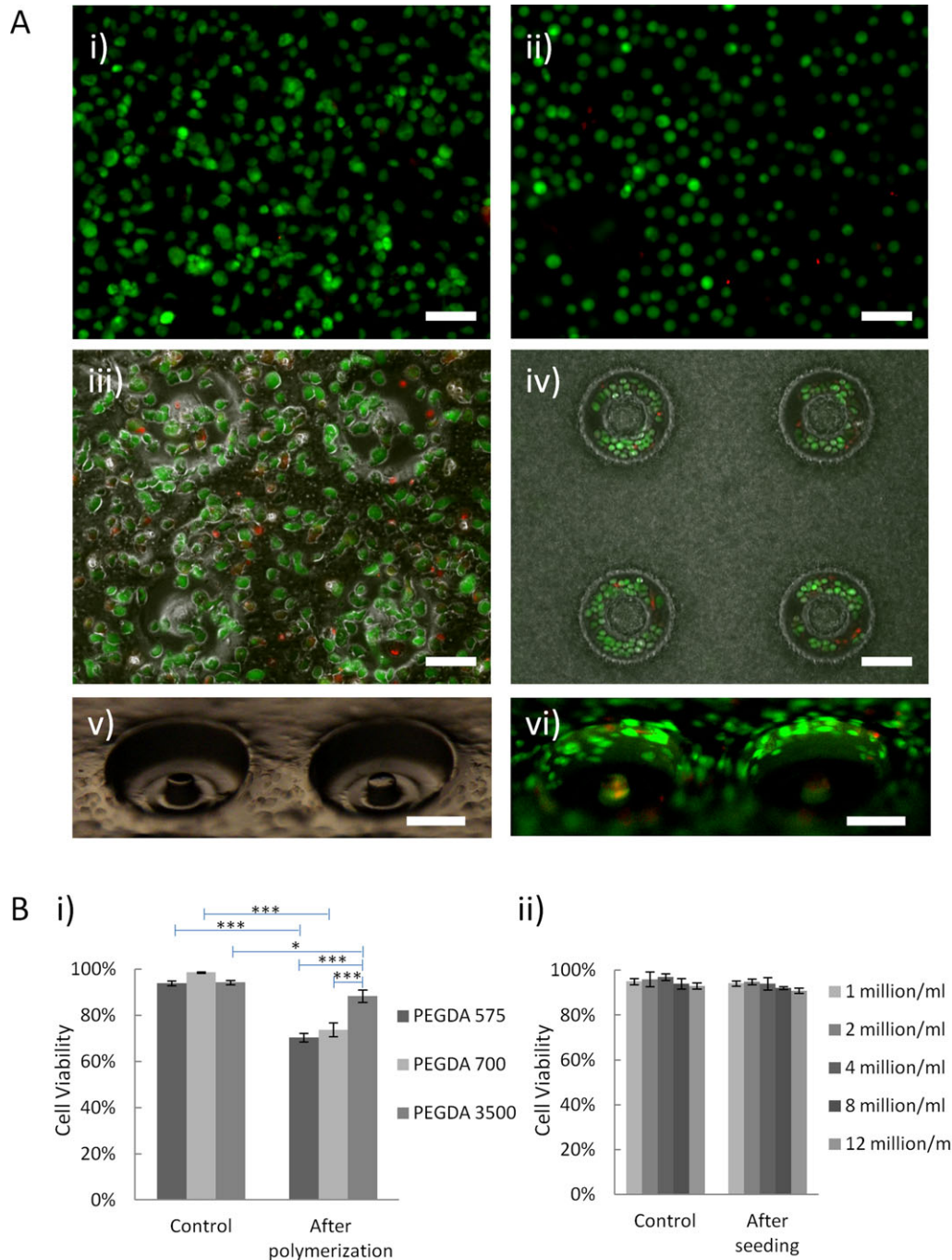


FIGURE 5. Encapsulating HDF cells (2×10^6 cells/mL) within microwell arrays and seeding HaCaT cells (4×10^6 cells/mL) on the top of microwell arrays respectively. A: (i): Cell viability (HDF) of the control group before UV exposure. (ii): Cell viability (HaCaT) of the control group before cell seeding. (iii): Phase and fluorescent superimposed image after applying a Live/Dead assay to HDF cells which demonstrates HDF cells were distributed uniformly in the gel. (iv): Phase and fluorescent superimposed image after applying a Live/Dead assay to HaCaT cells which demonstrates HaCaT cells were located in microwells. (v): 3D cell-laden microstructures. (vi): HDF cells stained with Ethd (red) and calcein-AM (green) in the 3D microstructure. B: (i): Cell viability in various MW PEGDA hydrogels. Cell viability of PEGDA hydrogels after microwell fabrication increased with increasing MW. PEGDA 575, PEGDA 700, and PEGDA 3500 were highly hydrated polymers containing 10% PEGDA in PBS. (ii): Cell viability before and after cell seeding showed no significant difference. Initial cell concentrations ranged from 1 to 12 million cell per mL. * and *** indicate $p < 0.05$ and $p < 0.001$ as compared to the viability of corresponding control group ($n = 3$). All scale bars represent $100 \mu\text{m}$. [Color figure can be viewed in the online issue, which is available at wileyonlinelibrary.com.]

prepolymer, each of which is known to influence the viability of cells negatively when used at concentrations higher than a threshold.⁴⁴ The toxicity of UV light, photoinitiator,

and PEGDA prepolymer on encapsulated cells was investigated, respectively. First, from the stability test, 10 and 20% (w/v) PEGDA are preferable in cell-laden microwell

fabrication. Therefore, HDF cells were subjected to 10 and 20% (w/v) PEGDA solutions (PEGDA 575, PEGDA 700, and PEGDA 3500) for 2 h. It was found that PEGDA solution of lower molecular weight was more cytotoxic to HDF and HDF cells in PEGDA 3500 solution survived longer [Supporting Information Fig. 2(A)]. Secondly, to minimize the toxicity of UV light, the minimum duration of UV exposure at various UV intensities was established, which was deemed to be the time required for the microwell array formation with no deformation. Then, HDF cells in PBS solution were exposed to UV for minimum duration to analyze the effect of UV alone. For the analysis of photoinitiator, HDF cells were suspended in 0.2% (w/v) photoinitiator for 2 h. The results showed that UV exposure and photoinitiator did not affect HDF viability on their own [Supporting Information Fig. 2(B,

C)]. Subsequently, each combination of UV intensity, PEGDA solution and photoinitiator were tested and the optimal conditions for cell-laden microwell fabrication were found to be 10% (w/v) PEGDA in 0.2% (w/v) photoinitiator under 4.96 W/cm^2 for 30 s. After cell encapsulation, the difference of cell viability among different MW PEGDA may be due to an increase in the free radical concentration produced from the shorter chained PEGDA 575 and PEGDA 700 during the crosslinking process. Furthermore, PEGDA 575 and PEGDA 700 allowed higher diffusion rates into the cells compared to PEGDA 3500 which can adversely affect cell viability.⁴⁵ For HaCaT cells, various cell densities (1–12 million cells per mL) were applied on the top of microwells. Cells were originally dispersed in the cell solution before cell seeding [Fig. 5(A-ii)] while cells were retained in microwells after

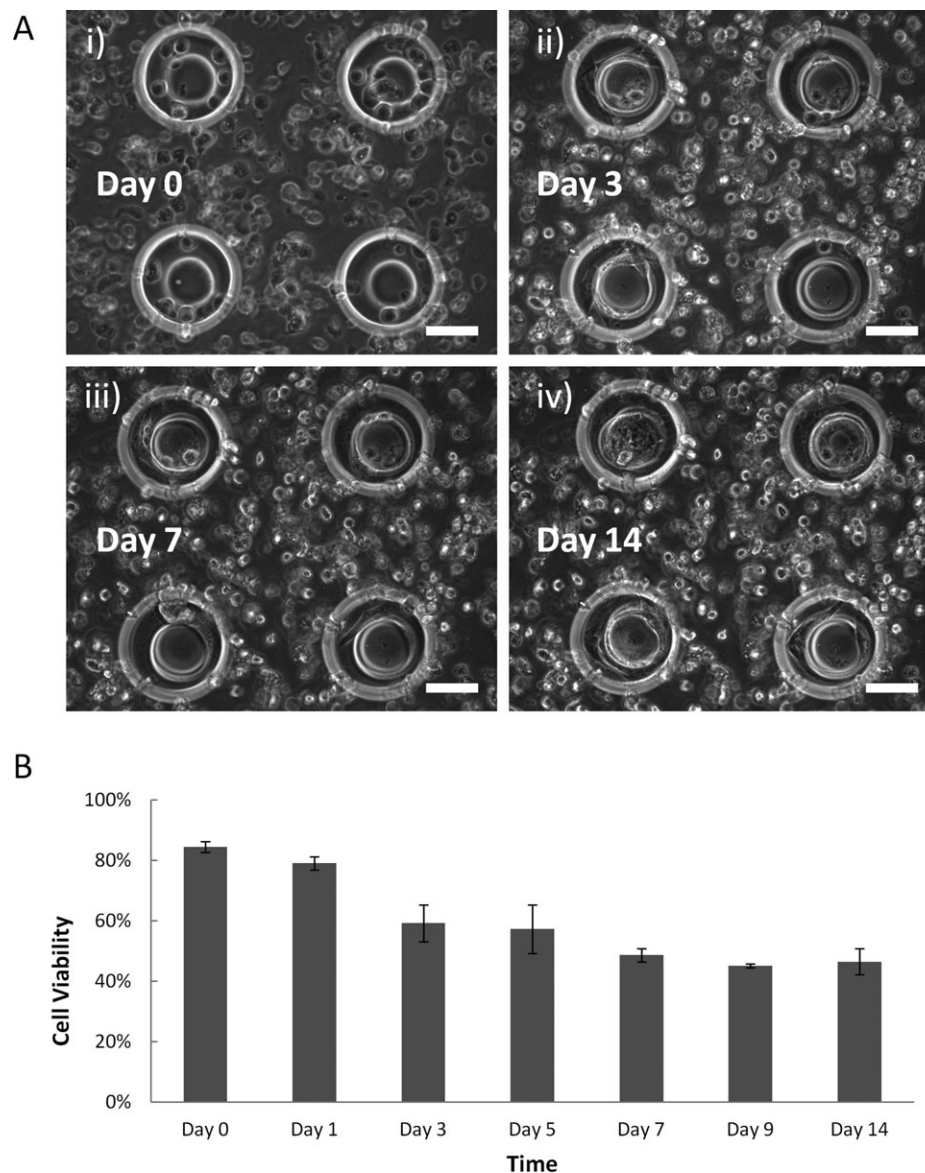


FIGURE 6. HDF cell encapsulation in PEGDA 3500 hydrogel over 2 weeks. A: (i–iv): Phase contrast images of HDFs in microgels. After 72 h, cell spreading was seen in the hydrogel and the morphology of cells continued to change over 2 weeks. Except Day 0, images of Day 3, Day 7, and Day 14 were from the same location of the hydrogel. B: Quantification of cell viability by Live/Dead assay over 2 weeks. Cell viability decreased consecutively on first 7 days, and then cell viability remained stable from Day 7 onwards around 48%. All scale bars represent $100 \mu\text{m}$.

cell seeding [Fig. 5(A-iv)]. After Live/Dead assay, cell viability of control group (before cell seeding) and experiment group (after cell seeding) had no significant difference [Fig. 5(B-ii)]. From the superimposed image, it was shown that HaCaT cells were localized inside the microwells after seeding [Fig. 5(A-iv)]. The diameter of HDF cells ($17.37 \pm 3.30 \mu\text{m}$) was larger than that of HaCaT cells ($10.77 \pm 2.04 \mu\text{m}$) and the diameter of HDF cells after cell encapsulation was $19.75 \pm 3.46 \mu\text{m}$ (Supporting Information Fig. 3). HDF cell attachment may be developed inside the micro-mould which leads to the size difference before and after cell encapsulation. It was demonstrated that two different types of cells can be controlled at the designated locations of microwell arrays, where HDF cells were uniformly distributed inside the fabricated gels and HaCaT cells were seeded on the top of microwells.

After microwell fabrication, the cells encapsulated in the hydrogels were monitored for up to 14 days at the same locations. Cell spreading was observed at the bottom of microwells after 72 h incubation and the morphology of cells changed at Day 7 and Day 14 [Fig. 6(A)]. The reason that cell spreading only occurred at the bottom of the microwell may be that the bottom was made of a thinner layer of PEGDA hydrogel which can minimize diffusion limitations and provide more effective nutrient transport.^{20,37} PEGDA 3500 in our study showed long-term viability for cells encapsulated over 14 days. From Live/Dead assays, it was shown that cell viability decreased quickly in first 3 days from 84.4 to 59.2%, while it was stabilized around 48% from Day 7 to Day 14 [Fig. 6(B)]. The initial decrease in cell viability could be due to cell damage caused by residual photocrosslinking factors encapsulated in hydrogels, such as toxic free radicals formed during crosslinking process, unpolymerized photoinitiator, and PEGDA monomers. These toxic factors may continuously diffuse into outside culture medium and eventually be removed after fresh medium was added repeatedly. As a result, the cell viability was maintained at the same level after 7 days. It has been reported that the addition of other factors into PEGDA gels can further improve cell development^{46,47} and this could be explored for future studies.

CONCLUSION

In this study, a 3D microstructure was fabricated by using a patterned PDMS stamp on a glass substrate. We demonstrated that 10 and 20% (w/v) PEGDA hydrogel microstructures are stable on the glass substrate and their mechanical properties were characterized by nano-indentation. HDF and HaCaT cells were immobilized at the designated locations of the microstructure, respectively. The number of HaCaT cells in the microwell increased with increasing cell density and cell seeding process did not compromise HaCaT cell viability. We also demonstrated that HDF survived inside the hydrogels over 14 days with observable cell spreading. Hence, this microstructure can be potentially used for human hair follicle regeneration *in vitro*.

ACKNOWLEDGMENTS

J. Pan is a recipient of the National University of Singapore Research Scholarship. We thank SBIC-Nikon Imaging Centre for providing the SMZ 1500 microscope for microwell imaging. A. Miserez and S. Amini thank the support of the Singapore National Research Foundation (NRF Fellowship to A. Miserez). The authors declare no conflict of interest.

REFERENCES

1. Krause K, Foitzik K. Biology of the hair follicle: the basics. *Semin Cutan Med Surg* 2006;25:2–10.
2. Annika Vogt KJM, Ulrike Blume-Peytavi. Biology of the hair follicle. In: David A, Whitting UB-P, Antonella Tosti and Ralph M. Trüeb, editor. *Hair Growth and Disorders*. Springer-Verlag: Berlin; 2008. p 1–22.
3. Stenn K, Parimoo S, Zheng Y, Barrows T, Boucher M, Washenik K. Bioengineering the hair follicle. *Organogenesis* 2007;3:6–13.
4. Leyden J, Dunlap F, Miller B, Winters P, Lebwohl M, Hecker D, Kraus S, Baldwin H, Shalita A, Draelos Z. Finasteride in the treatment of men with frontal male pattern hair loss. *J Am Acad Dermatol* 1999;40:930–937.
5. Messenger AG, Rundegren J. Minoxidil: Mechanisms of action on hair growth. *Br J Dermatol* 2004;150:186–194.
6. Orentreich N. Autografts in alopecias and other selected dermatological conditions. *Ann N Y Acad Sci* 1959;83:463–479.
7. Epstein JS. Evolution of techniques in hair transplantation: A 12-year perspective. *Facial Plast Surg* 2007;23:51–60.
8. Millar SE. Molecular mechanisms regulating hair follicle development. *J Invest Dermatol* 2002;118:216–225.
9. Stenn KS, Paus R. Controls of hair follicle cycling. *Physiol Rev* 2001;81:449–494.
10. Chuong CM, Cotsarelis G, Stenn K. Defining hair follicles in the age of stem cell bioengineering. *J Invest Dermatol* 2007;127:2098–2100.
11. Weinberg WC, Goodman LV, George C, Morgan DL, Ledbetter S, Yuspa SH, Lichti U. Reconstitution of hair follicle development in vivo: Determination of follicle formation, hair growth, and hair quality by dermal cells. *J Invest Dermatol* 1993;100:229–236.
12. Zheng Y, Du X, Wang W, Boucher M, Parimoo S, Stenn K. Organogenesis from dissociated cells: Generation of mature cycling hair follicles from skin-derived cells. *J Invest Dermatol* 2005;124:867–876.
13. Ehama R, Ishimatsu-Tsujii Y, Iriyama S, Ideta R, Soma T, Yano K, Kawasaki C, Suzuki S, Shirakata Y, Hashimoto K. Hair follicle regeneration using grafted rodent and human cells. *J Invest Dermatol* 2007;127:2106–2115.
14. Jone LN, Pope FM. Isolation of intermediate filament assemblies from human hair follicles. *J Cell Biol* 1985;101:1569–1577.
15. Higgins CA, Richardson GD, Ferdinando D, Westgate GE, Jahoda CA. Modelling the hair follicle dermal papilla using spheroid cell cultures. *Exp Dermatol* 2010;19:546–548.
16. Hashimoto T, Kazama T, Ito M, Urano K, Katakai Y, Yamaguchi N, Ueyama Y. Histologic and cell kinetic studies of hair loss and subsequent recovery process of human scalp hair follicles grafted onto severe combined immunodeficient mice. *J Invest Dermatol* 2000;115:200–206.
17. Auchincloss H Jr, Sachs DH. Xenogeneic transplantation. *Annu Rev Immunol* 1998;16:433–470.
18. Cicchetti F, Fodor W, Deacon TW, van Horne C, Rollins S, Burton W, Costantini LC, Isacson O. Immune parameters relevant to neural xenograft survival in the primate brain. *Xenotransplantation* 2003;10:41–49.
19. Havlickova B, Biro T, Mescalchin A, Tschirschmann M, Mollenkopf H, Bettermann A, Pertile P, Lauster R, Bodo E, Paus R. A human folliculoid microsphere assay for exploring epithelial-mesenchymal interactions in the human hair follicle. *J Invest Dermatol* 2009;129:972–983.
20. Khademhosseini A, Langer R, Borenstein J, Vacanti JP. Microscale technologies for tissue engineering and biology. *Proc Natl Acad Sci USA* 2006;103:2480–2487.

21. Barron JA, Wu P, Ladouceur HD, Ringeisen BR. Biological laser printing: A novel technique for creating heterogeneous 3-dimensional cell patterns. *Biomed Microdevices* 2004;6:139–147.
22. Rolland JP, Maynor BW, Euliss LE, Exner AE, Denison GM, DeSimone JM. Direct fabrication and harvesting of monodisperse, shape-specific nanobiomaterials. *J Am Chem Soc* 2005;127:10096–10100.
23. Pan J, Chan SY, Lee WG, Kang L. Microfabricated particulate drug-delivery systems. *Biotechnol J* 2011;6:1477–1487.
24. Kane RS, Takayama S, Ostuni E, Ingber DE, Whitesides GM. Patterning proteins and cells using soft lithography. *Biomaterials* 1999;20:2363–2376.
25. Koh WG, Revzin A, Pishko MV. Poly(ethylene glycol) hydrogel microstructures encapsulating living cells. *Langmuir* 2002;18:2459–2462.
26. Dendukuri D, Gu SS, Pregon DC, Hatton TA, Doyle PS. Stop-flow lithography in a microfluidic device. *Lab Chip* 2007;7:818–828.
27. Langer R, Vacanti JP. Tissue engineering. *Science* 1993;260:920–926.
28. Place ES, George JH, Williams CK, Stevens MM. Synthetic polymer scaffolds for tissue engineering. *Chem Soc Rev* 2009;38:1139–1151.
29. Zhu J. Bioactive modification of poly(ethylene glycol) hydrogels for tissue engineering. *Biomaterials* 2010;31:4639–4656.
30. Xia Y, Whitesides GM. Soft lithography. *Annu Rev Mater Sci* 1998;28:153–184.
31. Nichol JW, Koshy ST, Hojaj B, Hwang CM, Yamanlar S, Khademhosseini A. Cell-laden microengineered gelatin methacrylate hydrogels. *Biomaterials* 2010;31:5536–5544.
32. Kang L, Hancock MJ, Brigham MD, Khademhosseini A. Cell confinement in patterned nanoliter droplets in a microwell array by wiping. *J Biomed Mater Res A* 2010;93:547–557.
33. Zhang H, Wang L, Song L, Niu G, Cao H, Wang G, Yang H, Zhu S. Controllable properties and microstructure of hydrogels based on crosslinked poly(ethylene glycol) diacrylates with different molecular weights. *J Appl Polym Sci* 2011;121:531–540.
34. Revzin A, Russell RJ, Yadavalli VK, Koh WG, Deister C, Hile DD, Mellott MB, Pishko MV. Fabrication of poly(ethylene glycol) hydrogel microstructures using photolithography. *Langmuir* 2001;17:5440–5447.
35. Antony B. Mechanisms of membrane curvature sensing. *Annu Rev Biochem* 2011;80:101–123.
36. McMahon HT, Gallop JL. Membrane curvature and mechanisms of dynamic cell membrane remodelling. *Nature* 2005;438:590–596.
37. Moeller HC, Mian MK, Shrivastava S, Chung BG, Khademhosseini A. A microwell array system for stem cell culture. *Biomaterials* 2008;29:752–763.
38. Peppas NA, Brannon-Peppas L. Hydrogels at critical conditions. Part 1. Thermodynamics and swelling behavior. *J Membr Sci* 1990;48:281–290.
39. Temenoff JS, Athanasiou KA, LeBaron RG, Mikos AG. Effect of poly(ethylene glycol) molecular weight on tensile and swelling properties of oligo(poly(ethylene glycol) fumarate) hydrogels for cartilage tissue engineering. *J Biomed Mater Res* 2002;59:429–437.
40. Jahoda CA, Horne KA, Oliver RF. Induction of hair growth by implantation of cultured dermal papilla cells. *Nature* 1984;311:560–562.
41. Shimizu H, Morgan BA. Wnt signaling through the beta-catenin pathway is sufficient to maintain, but not restore, anagen-phase characteristics of dermal papilla cells. *J Invest Dermatol* 2004;122:239–245.
42. Deyrieux AF, Wilson VG. In vitro culture conditions to study keratinocyte differentiation using the HaCaT cell line. *Cytotechnology* 2007;54:77–83.
43. Zorlutuna P, Jeong JH, Kong H, Bashir R. Stereolithography-based hydrogel microenvironments to examine cellular interactions. *Adv Funct Mater* 2011;21:3642–3651.
44. Panda P, Ali S, Lo E, Chung BG, Hatton TA, Khademhosseini A, Doyle PS. Stop-flow lithography to generate cell-laden microgel particles. *Lab Chip* 2008;8:1056–1061.
45. Mazzoccoli JP, Feke DL, Baskaran H, Pintauro PN. Mechanical and cell viability properties of crosslinked low- and high-molecular weight poly(ethylene glycol) diacrylate blends. *J Biomed Mater Res A* 2010;93:558–566.
46. Chan V, Zorlutuna P, Jeong JH, Kong H, Bashir R. Three-dimensional photopatterning of hydrogels using stereolithography for long-term cell encapsulation. *Lab Chip* 2010;10:2062–2070.
47. Xu K, Fu Y, Chung W, Zheng X, Cui Y, Hsu IC, Kao WJ. Thiol-ene-based biological/synthetic hybrid biomatrix for 3-D living cell culture. *Acta Biomater* 2012;8:2504–2516.